



## Versatile cationic lipids for siRNA delivery

Jeff Sparks<sup>\*</sup>, Gregory Slobodkin, Majed Matar, Richard Congo, David Ulkoski, Angela Rea-Ramsey, Casey Pence, Jennifer Rice, Diane McClure, Kevin J. Polach, Elaine Brunhoeber, Leslie Wilkinson, Kirby Wallace, Khursheed Anwer, Jason G. Fewell

EGEN Inc., 601 Genome Way, Huntsville AL 35806, United States

### ARTICLE INFO

#### Article history:

Received 12 September 2011

Accepted 5 November 2011

Available online 12 November 2011

#### Keywords:

siRNA delivery  
Lipid nanoparticle  
Lung delivery  
PEGylation  
Functionalization

### ABSTRACT

Exploitation of the RNA interference (RNAi) pathway offers the promise of new and effective therapies for a wide variety of diseases. Clinical development of new drugs based on this platform technology is still limited, however, by a lack of safe and efficient delivery systems. Here we report the development of a class of structurally versatile cationic lipopolyamines designed specifically for delivery of siRNA which show high levels of target transcript knockdown in a range of cell types in vitro. A primary benefit of these lipids is the ease with which they may be covalently modified by the addition of functional molecules. For in vivo applications one of the core lipids (Staramine) was modified with methoxypolyethylene glycols (mPEGs) of varying lengths. Upon systemic administration, PEGylated Staramine nanoparticles containing siRNA targeting the caveolin-1 (Cav-1) transcript caused a reduction of the Cav-1 transcript of up to 60%, depending on the mPEG length, specifically in lung tissue after 48 h compared to treatment with non-silencing siRNA. In addition, modification with mPEG reduced toxicity associated with intravenous administration. The ability to produce a high level of target gene knockdown in the lung with minimal toxicity demonstrates the potential of these lipopolyamines for use in developing RNAi therapeutics for pulmonary disease.

© 2011 Elsevier B.V. All rights reserved.

### 1. Introduction

The primary obstacle for nucleic acid-based therapeutics is the efficient delivery to target cells. RNA-based therapeutics, which can result in the sequence-specific reduction of gene expression, must be able to enter cells and become available to the RNA-induced silencing complex (RISC) in the cytosol [1,2]. Many different types of systems have been utilized to deliver small inhibitory RNA (siRNA) including synthetic cationic polymers, natural polysaccharides, micelles, RNA, peptide and antibody conjugates, and microparticles, however liposomal systems have proven to be the most effective in vivo to date [3–6]. Yet obstacles remain for in vivo applications including toxicity, restricted tissue targets, and lack of active targeting. The development of siRNA delivery systems which can overcome these limitations has been the subject of intense recent focus [7–11].

Cationic lipids have three general structural components: the cationic head group, the lipid tail(s), and the linkers that connect the two. Although these features are common to many different cationic lipids, a clear relationship between lipid structure and siRNA delivery activity remains a goal in the field. When designing new molecules, one way to separate the active variants from the

inactive variants is to synthesize a large group of related molecules and screen them [9,12]. Another technique is to use amino acids or their side chain components as the basis for head group design, thereby employing the unique chemical entities utilized by nature in proteins and peptides to achieve biological function [13–16]. Alternatively, once an active molecule is identified, its constituents may be incrementally varied in order to optimize its properties [10]. Our approach has been to utilize structural motifs from highly active polyethylenimine (PEI)-based delivery systems which are being used for plasmid DNA and siRNA delivery and adapting them toward conventional lipid structures. PEI has a higher charge density than other conventional polymers used in transfection such as polylysine [17] and chitosan [18], and it is this property which is thought to cause the “proton sponge effect” [19], a key component of the endosomal escape process of internalized particles. Under physiological conditions, the pK<sub>a</sub> values for PEI amines can vary and drop substantially depending on the protonation state of neighboring amine groups due to charge repulsion [20]. This close-proximity theory has also been advanced for small pseudo-linear PEI molecules such as spermine in the context of DNA delivery [21]. Branched PEI contains roughly 25% tertiary amine groups which have pK<sub>a</sub>s of approximately 7, and it is thought that the majority remains unprotonated and become protonated only when the pH drops within the endosome. The presence of a tertiary amine within the lipid head group is thought to be a necessary structural component for some cationic

<sup>\*</sup> Corresponding author. Tel.: +1 256 327 0524; fax: +1 256 327 0988.  
E-mail address: [jsparks@egeninc.com](mailto:jsparks@egeninc.com) (J. Sparks).

lipids [10]. The general alkyl amine structural motif of PEI was used to generate symmetric cationic lipid analogs which form liposomal assemblies upon formulation and which retain the beneficial transfective properties of PEI. Liposomes composed entirely of these core structures can produce nanocomplexes that have very high transfection activity. In addition, a distinct design feature of these lipids is the presence of at least one primary amine group that is available for covalent attachment of modifiers such as small molecules, serum stabilizers, and targeting ligands. This inherent versatility allows the generation of formulations with a wide range of potential properties and does not require the co-formulation of commercial helper or PEG-lipids. Through rational design, we have developed a series of lipopolyamines that are distinguished by the number of reactive groups available for modification, having either one (Staramine) or two (Crossamine) such groups. Here we describe the synthesis of these systems and the evaluation of their ability to deliver siRNA in vitro and in vivo.

## 2. Materials and methods

Unless otherwise indicated, all solvents were HPLC-grade and purchased from ThermoFisher Scientific (Waltham, MA) and all compounds purchased from Sigma-Aldrich (St. Louis, MO).

### 2.1. Lipopolyamine synthesis

#### 2.1.1. Staramine

Oleoyl chloride (250 mmol) was heated at reflux with trifluoroethanol (600 mmol) for 16 h. After the evolution of HCl ceased, excess trifluoroethanol was removed under vacuum. Vacuum distillation of the residue afforded trifluoroethyl oleate (241 mmol) as colorless liquid. Yield = 96%. Boiling point 148–152 °C (at 0.3 mm Hg); NMR (CDCl<sub>3</sub>): δ 5.37 (m, 2H), 4.5 (m, 2H), 2.15 (t, 2H), 2.01 (m, 4H), 1.68 (m, 2H), 1.35 (m, 24H), 0.9 (t, 3H) (Fig. 1).

Tris-(2-aminoethyl)amine (10 mmol) was dissolved in 20 mL of ethanol. To this solution trifluoroethyl oleate (15 mmol) was added, and the reaction mixture was refluxed for 24 h. The mixture was concentrated under vacuum, the residue dissolved in 90% acetonitrile/10% water mixture and then acidified to pH 2–3 with trifluoroacetic acid (TFA). The crude mixture was split into seven aliquots and purified using an Biotage Isolera One system with a reverse phase C<sub>8</sub> silica (Fluka, 400 g) column cartridge (eluent consisted of a linear gradient from 49.9% acetonitrile/50% water/0.1% TFA to 89.9% acetonitrile/10% water/0.1% TFA over 15 column volumes). The purification afforded N, N'-dioleoyl tris(2-aminoethyl)amine (Staramine) (3 mmol) as its TFA salt. Yield = 23%. HPLC: single peak eluted at 5.5 min (Supplementary Fig. 1). MS (TFA salt): 675 [M + 1]; NMR (CDCl<sub>3</sub>): δ 5.37 (m, 4H), 3.55, 3.37 and 3.05 (poorly resolved, 12H total), 2.15 (t, 4H), 2.01 (m, 8H), 1.68 (m, 4H), 1.35 (m, 48H), 0.9 (t, 6H).

Detection and quantification of Staramine samples were carried out by analytical HPLC (Agilent, Santa Clara, CA). Separation was performed at 25 °C on a Zorbax SB-CN 5 μm particle, 4.6 × 250 mm column (Agilent). The mobile phase consisted of 69.9% acetonitrile/30% water/0.1% TFA. Chromatographic separation was performed at 1 mL/min and monitored at 205 nm (Agilent-1100 UV detector) and a PL-ELS-2100 detector. The nebulizer was set at 50 °C, the evaporator at 70 °C, and the ultra-high purity nitrogen gas flow rate at 1.6 slpm. Data collection and analysis were performed using ChemStation software (Agilent).

#### 2.1.2. Staramine derivatives

Methoxypolyethyleneglycol (mPEG) (polydisperse, average MW = 550 Da, approximately 12 ethylene glycol repeating units; 1.30 mmol) was dissolved in 8 mL of dry toluene. To this solution was added phosgene solution in toluene (4 mL of a 2 M solution, 8 mmol). The reaction mixture was stirred at room temperature for 3 h, then concentrated in vacuum at room temperature to afford

1.30 mmol of crude mPEG550 chloroformate. mPEG550 chloroformate (1.30 mmol) was dissolved in 6.313 g of dry methylene chloride and 5.66 g of this solution (1.04 mmol mPEG550 chloroformate) was added to a rapidly stirred solution of Staramine free base (1.04 mmol in 6 mL methylene chloride). The mixture was stirred for 3 h at room temperature, then concentrated and purified chromatographically using normal phase silica (50 g) with 3, 5, 10, and 15% methanol in methylene chloride (200 mL each) elutions. Reaction progress and purification was monitored by HPLC. The purification afforded Staramine-mPEG550 (0.664 mmol). Yield = 51%. HPLC: multiple peaks corresponding to Staramine-mPEG conjugates derived from each individual mPEG species eluted between 6 and 8 min, centered around 7 min (Supplementary Fig. 1). MS (TFA salt): multiple molecular weights observed in increments of 44 centered around 1192 [M + 2]. NMR (CDCl<sub>3</sub>): δ 5.37 (m, 4H), 4.15 (t, 2H), 3.6 (m, ~48H), 3.5 (t, 2H), 3.3 (s, 3H), 3.55, 3.37 and 3.05 (poorly resolved, 12H total), 2.15 (t, 4H), 2.01 (m, 8H), 1.68 (m, 4H), 1.35 (m, 48H), 0.9 (t, 6H) (Fig. 1). Staramine-mPEG2000 was synthesized in an analogous manner. Staramine-Cy5 was generated likewise using Cy5-NHS (Lumiprobe, Hallandale Beach, FL).

#### 2.1.3. Crossamine

Tetrakis(aminomethyl)methane tetrahydrochloride was prepared by a known procedure [12]. A 50 mL flask was charged with tetrakis(aminomethyl)methane tetrahydrochloride (2.88 mmol), methanol (10 mL) and sodium methoxide/methanol solution (2.10 g of 5.457 Molal, 11.50 mmol). The mixture was stirred and refluxed for 16 h then cooled. The methanol solution was decanted from the inorganic salts and the salts resuspended in 15 mL of absolute ethanol. The suspension was centrifuged and the combined supernatant solutions concentrated under vacuum. The residue was dissolved in 15 mL of methylene chloride and filtered from the remaining inorganic salts using a syringe filter (0.45 μm). Concentration of the filtrates afforded free tetrakis(aminomethyl)methane in a quantitative yield as a white semi-solid material (the residual solvents were estimated by NMR). NMR (D<sub>2</sub>O): δ 2.9 (s, CH<sub>2</sub>).

Tetrakis(aminomethyl)methane (2.86 mmol) was dissolved in 15 mL of absolute ethanol to which TFA (3.50 mmol) and 2,2,2-trifluoroethyl oleate (5.72 mmol) were added (see Staramine preparation). The homogeneous mixture was allowed to react for 72 h at room temperature, and then concentrated under vacuum. The residue was dissolved in methanol/water (10%)/TFA (0.1%) (40 mL) and the pH adjusted to 2 with TFA. The residue was purified by preparative HPLC on C<sub>8</sub> silica, using 89.6% methanol/10% water/0.4% TFA as eluent. N,N'-dioleoyl tetrakis(aminomethyl)methane (Crossamine) was isolated as the bis-TFA salt (1.01 mmol). Yield = 35%. HPLC: single peak eluted at 17.5 min (Supplementary Fig. 1). MS: (bis-TFA salt) 661 [M + 1]; NMR (CDCl<sub>3</sub>): δ 5.37 (m, 4H), 3.07 and 2.95 (poorly resolved, 4H each); 2.15 (t, 4H), 2.01 (m, 8H), 1.35 (m, 48H), 0.9 (t, 6H) (Fig. 1).

Detection and quantification of Crossamine samples were carried out by analytical HPLC (Agilent). Separation was performed at 25 °C on a Zorbax XDB-C<sub>8</sub> 5 μm particle, 4.6 × 150 mm column (Agilent). The mobile phase consisted of 89.6% methanol/10% water/0.4% TFA. Chromatographic separation and data collection remained the same as in the Staramine assay.

#### 2.1.4. Formulation of Staramine liposomes and siRNA cargo

siRNAs targeting luciferase and the non-silencing controls were purchased from ThermoFisher Scientific (siSTABLE). The sequences are as follows: siNon sense: 3'-UGGUUUACAUGUCGACUAAUU-5'; siNon antisense: 5'-UUAGUCGACAUGUAAACCAU-3'; siLuc sense: 3'-CGUACGCGAAUACUUCGAUU-5'; siLuc antisense: 5'-UCGAGUAAUCCGCUACGUU-3'. siRNA targeting β-actin were purchased from ThermoFisher Scientific (siGENOME SMARTpool) and were an equal mixture of four siRNAs (sense): 3'-GAAUUCGUGCGUGACAUUA-5'; 3'-

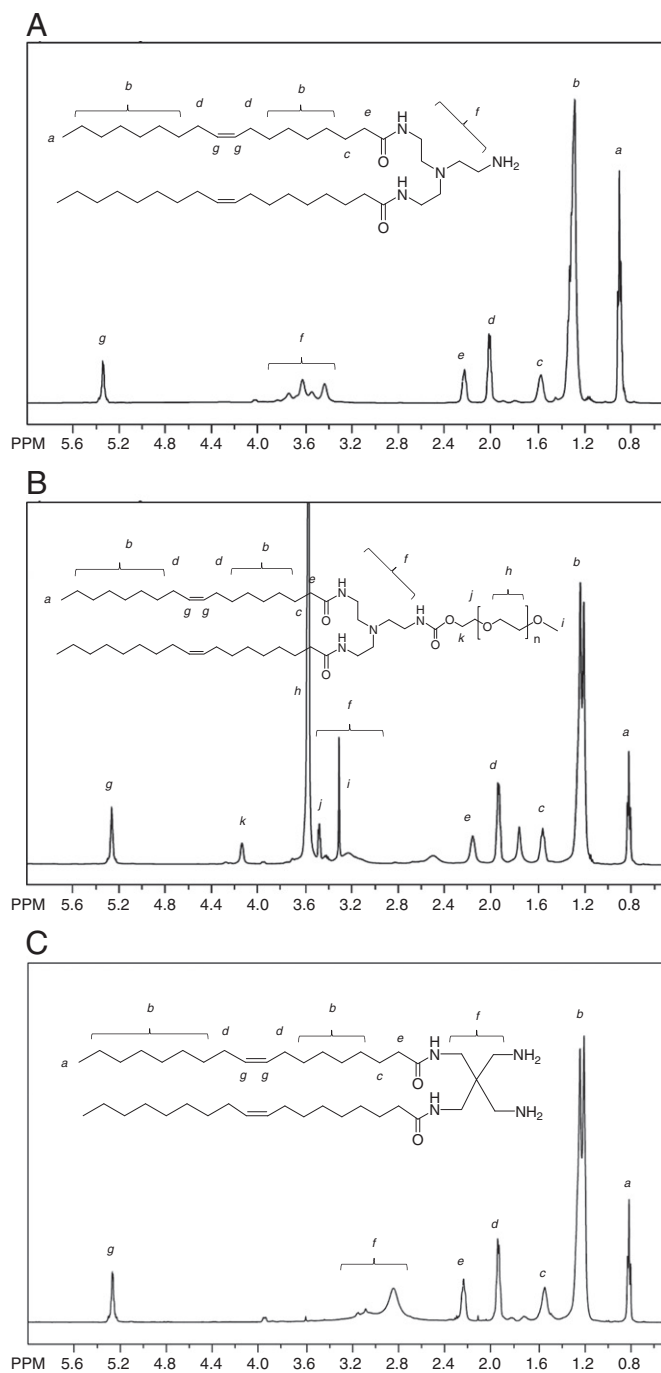


**Fig. 1.** Lipid structures and <sup>1</sup>H NMR peak assignments. (A) Staramine (B) Staramine-mPEG (C) Crossamine. Based on the manufacturer's specified molecular weight for each PEG species, for mPEG550, n = ~12; for mPEG2000, n = ~45.

GGGCAUGGGUCAGAAGGAU-5'; 3'-AAACCUAACUUGCGCAGAA-5'; 3'-ACUUGAGACCAGUUGAAUA-5'. Chloroform solutions of Staramine or Crossamine alone or 10:1 mixtures of Staramine and Star-mPEG550 or Staramine-mPEG2000 were rotary-evaporated to a film. The flask containing this film was held under high vacuum overnight. Water for injection (B. Braun Medical Inc., Irvine, CA) was then added to the film to give the desired Staramine concentration. This suspension was sonicated in a bath for approximately 30 min followed by a probe sonication for 5 min using a continuous pulse sonication with 5–10 watt output (ThermoFisher Scientific, Sonic Dismembrator, Model 100). The liposome solution was then filtered through a 0.2 μm filter. The liposome solution was diluted with 5% dextrose and mixed with the desired amount of siRNA. Particle size and zeta potential measurements were

conducted using Brookhaven 90 Plus Particle Size and Zeta Potential Analyzer (Brookhaven Instruments, Holtsville, NY).

#### 2.1.5. Serum studies

Staramine, Staramine:Staramine-mPEG550, and Staramine:Staramine-mPEG2000 (10:1) nanocomplexes were prepared at an siRNA concentration of 0.1 mg/mL (N:P = 20:1) in 5% dextrose. For turbidity assessment, samples were diluted 1:1 in serum and incubated at 37 °C. Each reading was blanked against 50% serum in 5% dextrose and absorbance measured at 600 nm at each time point. For particle size assessment, readings of freshly prepared samples were taken without serum (–5 min), then dilutions were made into 10% serum

where remaining readings were taken (0, 1, 5 min). The reported values are the average of two readings.

#### 2.1.6. *In vitro* transfection assays

Twenty four hours prior to transfection, MB49 cells (murine bladder carcinomas, kindly provided by Dr. Yi Luo, University of Iowa), which stably express firefly luciferase, were plated in a 24-well plate at an approximate density of  $8 \times 10^4$  cells per well. On the day of transfection a Staramine nanocomplex solution was prepared by mixing the siRNA (siLuc or non-silencing control) solution (1  $\mu$ L of a 1 mg/mL solution of siLuc or siNon in 99  $\mu$ L of 5% dextrose) with the Staramine solution (25  $\mu$ L of a 1 mg/mL solution of Staramine liposomes prepared as above in 75  $\mu$ L of 5% dextrose). Dilutions (50  $\mu$ L, 25, 12.5, 6.25, 3) of the nanocomplex solution were made in 5% dextrose (total volume 50  $\mu$ L). Fifty microliters of the Staramine nanocomplex solutions were added to 200  $\mu$ L of 12.5% FBS in RPMI media to give a total volume of 250  $\mu$ L, which were then added to each previously aspirated well of a 24 well plate. After the plate was incubated at 37 °C (5% CO<sub>2</sub>) for 4 h, 250  $\mu$ L of additional 10% FBS were added to each well. The plate was then incubated for an additional 48 h, at which time the luciferase signal was measured using a microplate luminometer (Berthold Detection Systems, Huntsville, AL). Cell lysates (20  $\mu$ L per sample) were analyzed by BCA protein assay (ThermoFisher Scientific) to determine total protein according to the manufacturer's instructions. K562 (human bone-marrow-derived lymphoma cells, ATCC) cells were plated to a density of approximately 200,000 cells/well in 24-well culture plate. si $\beta$ -actin or a non-silencing control (0.25  $\mu$ g) were complexed with Crossamine at (20:1) N:P ratio in 5% dextrose. The transfection complex was added to cells in presence of 10% FBS. Cells were incubated for 48 h before the gene knockdown assay was performed. Fluorescence assays were performed with Staramine or Crossamine nanocomplexes containing 1% of Cy5-labeled Staramine, complexed with FITC-siRNA. MB49 and A549 (human lung carcinoma cells, ATCC) cells (1 mL of cell suspension) were plated into each chamber of a chamber slide at a concentration of  $7.5 \times 10^4$  cells/mL in growth media. After 24 h, the cells were transfected as above. Four hours after transfection cells were washed and fixed/stained, then viewed at 40 $\times$  magnification using a Zeiss Axiovert 40 CFL microscope.

#### 2.1.7. LDH assay

An LDH assay (CytoTox-ONE, Promega, Madison, WI) was performed to assess the relative cytotoxicity of Staramine and Crossamine. Transfections were performed as above with the addition of 2% (v/v) Triton-X 100 as a positive control (maxLDH). After the cells were treated with Staramine or Crossamine nanocomplexes, or with Triton-X 100, cells were incubated at 37 °C at 5% CO<sub>2</sub> for 4 h. The supernatant from each well (250  $\mu$ L) was collected and centrifuged at 10,000 rpm for 5 min. To a black 96-well plate was added 100  $\mu$ L of each supernatant in duplicate. To each well containing supernatant was added 100  $\mu$ L of substrate solution (11.25 mL assay buffer in one vial of Substrate Mix). The plate was incubated in the dark at room temperature for 10 min and was then read in a fluorescence plate reader at an excitation wavelength of 560 nm and an emission wavelength of 590 nm. Percent cytotoxicity was calculated according to the formula: [(sample-background)/(maxLDH-background)  $\times$  100]. The amount of LDH detected is reported for decreasing amounts of siLuc relative to Triton X-100.

#### 2.1.8. Animals

All procedures used in animal studies were performed in accordance with local, state and federal regulations and approved by the Institutional Animal Care and Use Committee. Female ICR mice were obtained from Harlan Laboratories (Houston, TX) and ranged from 8 to 10 weeks of age (17–22 g) at the time of each study.

#### 2.1.9. *In vivo* gene silencing assays

siRNAs targeting Cav-1 and a non-silencing control sequence were purchased from Dharmcon (siSTABLE, *in vivo* purified) and contained the following sequences: siCav-1 sense: 3'-GUCCAUACCUUCUGCGAUCUU-5'; siCav-1 antisense: 5'-GAUCGCAGAAGG UAUGGACUU-3'; siRNA nanocomplexes were diluted into sterile water containing 5% dextrose and injected into the tail vein of female ICR mice. Injection doses were adjusted by altering the concentration of particles in each injection; injection volumes were held constant at 10  $\mu$ L/g. At various times post-injection, organs were collected and immediately frozen in liquid nitrogen for storage at -80 °C. Total RNA was collected from tissues using Tri-Reagent (Molecular Research Center, Cincinnati, OH) according to the manufacturer's protocol. These RNA stocks were used as templates for synthesis of complementary DNAs (cDNAs) using random hexamer primers and reverse transcriptase (Multiscribe, Applied Biosystems, Carlsbad, CA). The reverse transcription reaction contained: 10 mM Tris-HCl (pH 8.3), 50 mM KCl, 5.5 mM MgCl<sub>2</sub>, 50 ng total RNA, 2.5  $\mu$ M random hexamer primer, 500  $\mu$ M each dNTP, 0.4 unit/ $\mu$ L RNase inhibitor, 1.25 U/ $\mu$ L Reverse Transcriptase. TaqMan primers and probe sets (Applied Biosystems) were used in qPCR to amplify the transcript of interest from the corresponding cDNA template. The qPCR reaction contained: TaqMan Gene Expression Master Mix (Applied Biosystems), 50 ng cDNA, 900 nM forward and reverse primers, 250 nM FAM-labeled MGB probe. All changes were measured against an internal control using primers specific for housekeeping genes (GAPDH or Ppib).

### 3. Results and discussion

#### 3.1. Synthesis of Staramine, Crossamine, and their derivatives

The core Staramine and Crossamine lipopolyamines were designed to provide high levels of target gene knockdown while possessing structures which are readily modifiable. We chose head groups which had such molecular geometry as to potentially possess primary amine groups either in close proximity to tertiary amine groups or to one another (Fig. 1).

The synthetic linker was selected in order to maximize synthesis simplicity. The choice of acylating agent, a mildly activated trifluoroethyl ester, was dictated by the considerations of reactivity. The degree of its reactivity should be high enough for the reaction to proceed in a reasonably short time, but at the same time low enough to allow for the acylating agent to be dispersed in the reaction mixture. This precluded the use of functionalities such as acyl chlorides and chloroformates. Ultimately, the ease of the byproduct trifluoroethanol removal was a benefit of using trifluoroethyl activation. Although the nature of the lipid tail was not optimized, oleoyl-based lipids were chosen based on the large number of reports of their utility as components of nucleic acid delivery systems.

Structural versatility is a distinguishing design feature of these lipids. A primary goal was to reduce the total number of unique components required to generate active formulations. The majority of current therapeutic liposomal formulations are composed of a cationic lipid, a fusogenic lipid, a PEG-lipid and cholesterol. We felt that by designing a single highly active cationic lipid which has endosomolytic properties as well as the ability to be readily modified, we might gain utility in the simplicity of the formulation. Through covalent attachment of small molecule drugs, serum stabilizers, and targeting ligands, the properties of the resulting nanoparticles may theoretically be tuned to fit a specific delivery application or target a specific tissue or organ. As a validation of this structural advantage, we synthesized PEGylated derivatives of Staramine in order to control the *in vivo* properties of the lipopolyamine formulations.

#### 3.2. *In vitro* activity of Staramine and Crossamine nanoparticles

Staramine and Crossamine nanoparticles were formed using the thin film hydration method, and mixed with siRNA to form

nanocomplexes. Particle sizes ranged from 80–100 nm and zeta potentials ranged from 15–40 mV, depending on the formulation, and were a function of the N:P ratio and presence and/or length of mPEG in the composition. siRNA loading of >90% for both Staramine and Crossamine was routinely observed based on agarose gel electrophoresis. Staramine and Crossamine were tested in a large number of in vitro applications including adherent cell lines, suspension cell lines, and primary cells, and in some cases showed activity which was equal to or better than current popular commercial reagents (Supplementary Table 1, Supplementary Figs. 2 and 3). To demonstrate this activity, Staramine nanoparticles were complexed with siRNA targeting luciferase, and knockdown of luciferase was measured as a function of luciferase activity in MB49 cells using a Pro-mega Luciferase Assay System (Fig. 2A).

Crossamine was highly active in adherent, as well as suspension cell lines, including K562. Human  $\beta$ -actin transcript knockdown activity was measured as a function of siRNA concentration and greater than 90% reduction was found at siRNA concentrations as low as 5 nM

relative to a nonsilencing control (Fig. 2B). An LDH assay, used as a measure of cell lysis, also suggested there is very low cytotoxicity for both Staramine and Crossamine nanocomplexes across a wide range of transfection concentrations (Supplementary Fig. 4). Cy-5 labeled Staramine and Crossamine with FITC labeled siRNA were formulated to transfect MB49 and A549 cells (Fig. 2C). A much larger amount of FITC signal was observed in cells treated with Staramine and Crossamine (Fig. 2C, middle, right) compared to cells which were treated with FITC-siRNA alone (Fig. 2C, left). The diffuse staining of the siRNA and the Staramine and Crossamine indicates broad cytosolic distribution expected from formulations which result in high levels of transcript knockdown.

### 3.3. In vivo activity of Staramine nanoparticles

PEGylated lipids are utilized for in vivo applications within formulations in order to stabilize nanoparticles against serum components. Highly cationic nanoparticles are known to generate immune responses through interaction with blood components including proteins involved in the complement system, which leads to uptake and clearance by macrophages [22]. PEG is routinely added into nanoparticles to reduce the surface charge, and therefore toxicity, after systemic administration. This is normally accomplished through the covalent attachment of mPEG to phosphatidylethanolamine-based structures or through glycerol-based structures [7–9,12,23–26], and then by adding these lipids into mixtures of other lipids. Here we demonstrate the utility of using PEGylated Staramine molecules in the nanocomplexes to achieve efficient target gene knockdown in vivo while moderating toxicity. The primary amine of the Staramine head group was utilized as the attachment point for mPEG. Although the particle sizes for the PEGylated formulations remained relatively unchanged, the zeta potentials were reduced by 50%. In our system this was evidenced by a reduction in the toxicity index value (Fig. 3A) which is a rapid and convenient qualitative test of acute toxic response in mice. This parameter is based on cage side observations of animal reaction and behavior after dosing. Each animal was scored on a 1–5 scale (5 being sign of severe toxicity) in each of four categories, including respiration, posture, social interaction, and coat appearance. The scores for each animal were summed and this value recorded as the toxicity index. For this index values of 5 are indicative of moderate toxicity while values of <2 are indicative of little or no acute toxicity. Caveolin-1 (Cav-1), a protein involved in caveolae formation during endocytosis was selected as the target gene due to its widespread expression in most tissue. Mice were administered intravenously a single dose of unmodified Staramine/siCav-1 nanocomplexes (N:P 20:1) or nanocomplexes containing PEGylated Staramine with different length PEGs (500 and 2000 Da) incorporated into Staramine nanoparticles. The addition of PEG modification into the Staramine formulation served to dramatically reduce the observed toxicity index compared to Staramine alone (Fig. 3A). Additional confirmation of reduced toxicity was obtained from histopathology of lung tissue where it was seen that unmodified Staramine-treated mice displayed evidence of hemorrhagic foci with associated fibrin thrombi, while Staramine-mPEG550 mice showed lung tissue similar to untreated animals (Fig. 3B).

The effect of PEGylation on knockdown activity was also examined. Forty-eight hours after injection, significant Cav-1 transcript knockdown was found in the lung but not the liver for both Staramine and Staramine-mPEG550 formulations (Fig. 3C). The Staramine-mPEG550 maintained a ~40% siRNA target specific knockdown which was only slightly reduced compared to the nonPEGylated nanocomplexes (Fig. 3C). Although the addition of the longer mPEG2000 to Staramine (Staramine-mPEG2000) served to reduce the acute toxicity to the greatest extent (Fig. 3A), knockdown levels were moderately reduced relative to nonPEGylated and Staramine-mPEG550 nanocomplexes. Additional ratios of Staramine to Staramine-mPEG550 were tested, including both higher and lower

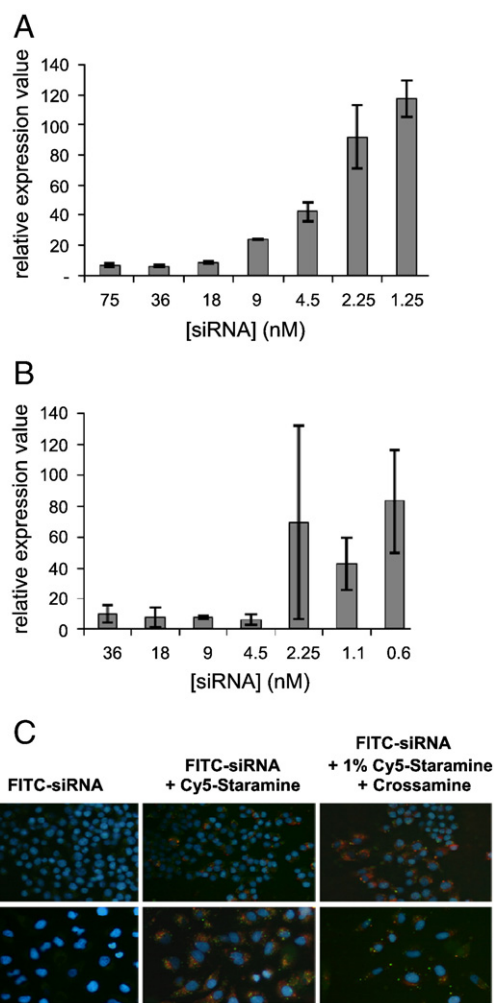


**Fig. 2.** In vitro target gene knockdown by Staramine and Crossamine nanocomplexes. (A) Luciferase expression was measured in MB49 cells after transfection with Staramine nanocomplexes containing siLuc or a non-silencing control. Knockdown for each concentration is reported relative to the non-silencing control value for that concentration. (B)  $\beta$ -actin expression was measured in K562 cells after transfection with Crossamine nanocomplexes containing si $\beta$ -actin or a non-silencing control. Knockdown for each concentration is reported relative to the non-silencing control value for that concentration. (C) MB49 (top row) and A549 (bottom row) cells were treated with nanocomplexes composed of FITC-labeled siRNA only (left), Staramine (+1% Cy5-labeled Staramine) nanocomplexes (center), or Crossamine (+1% Cy5-labeled Staramine) nanocomplexes (right). Nuclei are stained with DAPI. 40 $\times$  magnification. Values expressed are means  $\pm$  SD.

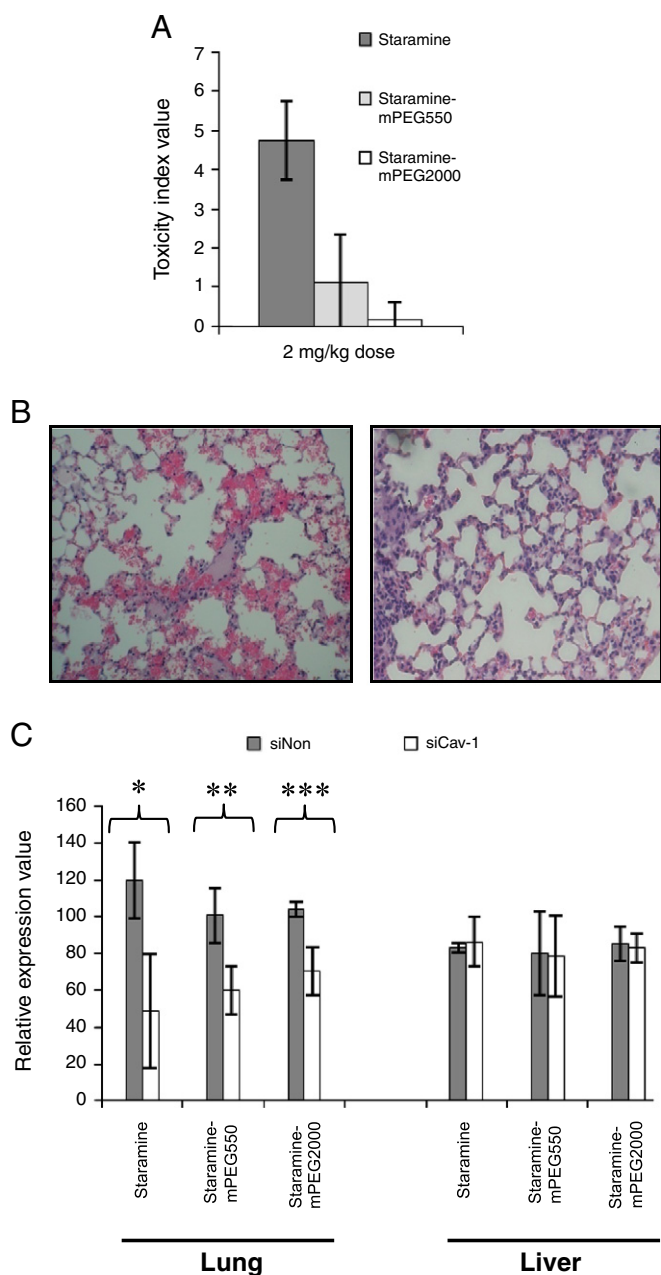


**Fig. 3.** In vivo activity of PEGylated Staramine nanocomplexes. Doses were 2.0 mg/kg siCav-1 (or non-silencing control) in 200  $\mu$ L; N:P = 20:1; ratio of Staramine-mPEG550 or Staramine-mPEG2000 to Staramine = 1:10. (A) Toxicity index was determined for Staramine, Staramine:Staramine-mPEG550, and Staramine:Staramine-mPEG2000 nanoparticles after a single iv dose. (B) Cross sections of lung tissue stained with hematoxylin and eosin after treatment with Staramine (left) and Staramine-mPEG550 (right) nanocomplexes. (C) Cav-1 transcript knockdown was determined in lungs and liver 48 h after a single iv dose of Staramine, Staramine-mPEG550, and Staramine-mPEG2000 nanoparticles.  $n = 5$  for each group. Values expressed are means  $\pm$  SD. \*  $P < 0.001$ , \*\*  $P < 0.007$ , \*\*\*  $P < 0.01$ .

ratios than those reported here, however these formulations either gave reduced levels of knockdown or increased levels of toxicity. In summary, it appears PEGylation serves to decrease acute toxicity with only a mild reduction in activity, and a 1:10 incorporation of Staramine-mPEG550 into Staramine nanocomplexes achieves a balance of activity and toxicity not found in the other combinations.

This Staramine mPEG550 formulation was the focus of further studies both involving target gene knockdown activity and toxicity. Cav-1 transcript knockdown was examined as a function of siCav-1 concentration from 10 to 100  $\mu$ g per dose (0.5–5.0 mg/kg) 48 h after

treatment (Fig. 4A). In addition, the amount of siCav-1 was measured in the lung tissue for each dose using a stem loop quantitative PCR assay.

Target transcript knockdown was found to increase with increasing siCav-1 detected, with the greatest target gene knockdown and siCav-1 found at a 5.0 mg/kg dose (Fig. 4A). In addition, all dosing levels were safe based in the toxicity index (Fig. 4B). Due to the observation that gross toxicity may be correlated with animal weight loss [24], animals were weighed 24 h after treatment (Fig. 4C). All doses below 3.0 mg/kg resulted in weight loss that was not significantly different from dextrose treatment.

Although not a new observation in regard to biodistribution of cationic nanocomplexes [27], this significant knockdown activity in the lung stands in contrast to the majority of cationic liposomes in current development for siRNA therapeutics which show uptake and gene knockdown activity primarily in the liver [7–10,12]. Interestingly, it is not immediately apparent why other PEGylated cationic liposomes which possess markedly similar properties show knockdown

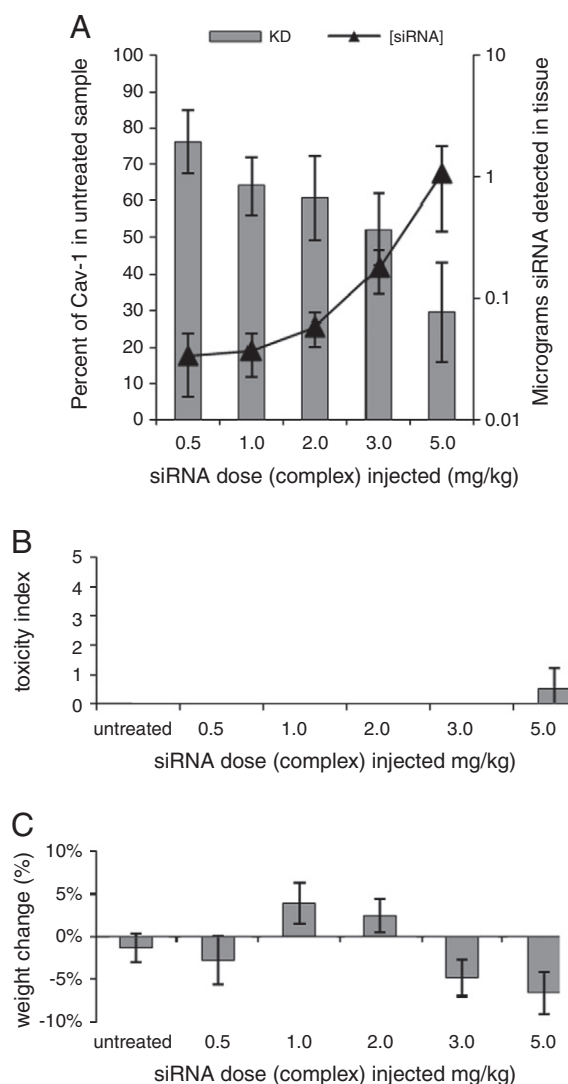


**Fig. 4.** In vivo activity of PEGylated Staramine nanocomplexes as a function of dose. Doses were 10, 20, 40, 60, 100  $\mu$ g siCav-1 (or non-silencing control) [which corresponds to 0.5, 1, 2, 3, or 5 mg/kg siCav-1 (or non-silencing control)] in 200  $\mu$ L; N:P = 20:1; ratio of Staramine-mPEG550 to Staramine = 1:10. (A) Cav-1 transcript knockdown in lung was determined relative to untreated animals 48 h after a single iv injection. The amount of siCav-1 in the tissue was determined for each dose. The toxicity index (B) and animal weight change (C) were evaluated for each dose.  $n = 5$  for each group. Values expressed are means  $\pm$  SD.

activity in the liver rather than the lung [24]. This effect could be explained, in part, by variable particle aggregation induced by serum components, which may lead to uptake in lung fenestration due to alteration of the particle size and surface properties [28]. However, PEGylation of the liposomes routinely serves as a modification to reduce such an effect [29–31], one which we have observed by measuring both turbidity and particle sizes in the presence of serum for Staramine-based formulations (Supplementary Figs. 5 and 6). In these assays, particle sizes observed for non-PEGylated Staramine increased significantly, which was reflected in the increase in turbidity. Although Staramine-mPEG550 nanocomplexes showed turbidity in serum that was similar to nonPEGylated Staramine, the particle sizes of the Staramine-mPEG550 nanocomplexes were impacted much less dramatically and were similar to Staramine-mPEG2000 nanocomplexes, which showed very little turbidity. The effect of the increased stability of the Staramine-mPEG550 formulation (as indicated by a maintained relatively small particle size) is most readily seen in the amount of siRNA found in tissues shortly after intravenous injection (Supplementary Fig. 7). The vast majority of material is found in the liver rather than the lung after 5 min. The nanocomplexes necessarily passed through the lung without entrapment prior to being taken up by the liver. In addition, we have demonstrated that Staramine-mPEG550 nanocomplexes achieve target gene knockdown in lung in part due to the significantly slower clearance rate of the siRNA from lung tissue relative to other tissues, which results in prolonged accumulation on the timescale of RNAi-mediated transcript depletion [32]. It is clear from these studies that PEGylation has a physical impact on the interaction of the nanocomplexes with serum, but the shielding effect provided by PEGylation only minimally reduces target gene knockdown.

#### 4. Conclusion

Two cationic lipids, Staramine and Crossamine, were synthesized with the goal of producing active and easily modifiable structures which could be formulated into nanoparticles for the delivery of siRNA. We have demonstrated the versatility of the compounds by functionalizing Staramine with mPEG. While both lipids exhibited high degrees of in vitro activity, Staramine was found to possess a high level of target gene knockdown in vivo. Its toxicity upon intravenous administration could be mitigated by the addition of PEGylated Staramine molecules to the formulation without significantly reducing knockdown activity. A thorough mechanistic investigation of this system is underway, including analysis of siRNA accumulation and elimination kinetics, as well as use in therapeutic applications such as pulmonary arterial hypertension and lung cancer.

#### Appendix A. Supplementary data

Supplementary data to this article can be found online at doi:10.1016/j.jconrel.2011.11.006.

#### References

- [1] R. Juliano, J. Bauman, H. Kang, X. Ming, Biological barriers to therapy with anti-sense and siRNA oligonucleotides, *Mol. Pharm.* 6 (2009) 686–695.
- [2] K.A. Whitehead, R. Langer, D.G. Anderson, Knocking down barriers: advances in siRNA delivery, *Nat. Rev. Drug Discov.* 8 (2009) 129–138.
- [3] M. Frank-Kamenetsky, A. Grefhorst, N.N. Anderson, T.S. Racie, B. Bramlage, A. Akinc, D. Butler, K. Charisse, R. Dorkin, Y. Fan, C. Gamba-Vitalo, P. Hadwiger, M. Jayaraman, M. John, K.N. Jayaprakash, M. Maier, L. Nechev, K.G. Rajeev, T. Read, I. Rohl, J. Soutschek, P. Tan, J. Wong, G. Wang, T. Zimmermann, A. de Fougerolles, H.P. Vornlocher, R. Langer, D.G. Anderson, M. Manoharan, V. Koteliensky, J.D. Horton, K. Fitzgerald, Therapeutic RNAi targeting PCSK9 acutely lowers plasma cholesterol in rodents and LDL cholesterol in nonhuman primates, *Proc. Natl. Acad. Sci. U. S. A.* 105 (2008) 11915–11920.
- [4] T.W. Geisbert, A.C. Lee, M. Robbins, J.B. Geisbert, A.N. Honko, V. Sood, J.C. Johnson, S. de Jong, I. Tavakoli, A. Judge, L.E. Hensley, I. MacLachlan, Postexposure protection of non-human primates against a lethal Ebola virus challenge with RNA interference: a proof-of-concept study, *Lancet* 375 (2010) 1896–1905.
- [5] T.S. Zimmermann, A.C. Lee, A. Akinc, B. Bramlage, D. Bumcrot, M.N. Fedoruk, J. Harborth, J.A. Heyes, L.B. Jeffs, M. John, A.D. Judge, K. Lam, K. McClintock, L.V. Nechev, L.R. Palmer, T. Racie, I. Rohl, S. Seiffert, S. Shanmugam, V. Sood, J. Soutschek, I. Toudjarska, A.J. Wheat, E. Yaworski, W. Zedalis, V. Koteliensky, M. Manoharan, H.P. Vornlocher, I. MacLachlan, RNAi-mediated gene silencing in non-human primates, *Nature* 441 (2006) 111–114.
- [6] A. Schroeder, C.G. Levins, C. Cortez, R. Langer, D.G. Anderson, Lipid-based nanotherapeutics for siRNA delivery, *J Intern Med* 267 (2010) 9–21.
- [7] M.T. Abrams, M.L. Koser, J. Seitzer, S.C. Williams, M.A. DiPietro, W. Wang, A.W. Shaw, X. Mao, V. Jadhav, J.P. Davide, P.A. Burke, A.B. Sachs, S.M. Stirdivant, L. Sepp-Lorenzino, Evaluation of efficacy, biodistribution, and inflammation for a potent siRNA nanoparticle: effect of dexamethasone co-treatment, *Mol. Ther.* 18 (2010) 171–180.
- [8] A. Akinc, W. Querbes, S. De, J. Qin, M. Frank-Kamenetsky, K.N. Jayaprakash, M. Jayaraman, K.G. Rajeev, W.L. Cantley, J.R. Dorkin, J.S. Butler, L. Qin, T. Racie, A. Sprague, E. Fava, A. Zeigerer, M.J. Hope, M. Zerial, D.W. Sah, K. Fitzgerald, M.A. Tracy, M. Manoharan, V. Koteliensky, A. Fougerolles, M.A. Maier, Targeted delivery of RNAi therapeutics with endogenous and exogenous ligand-based mechanisms, *Mol. Ther.* 18 (2010) 1357–1364.
- [9] K.T. Love, K.P. Mahon, C.G. Levins, K.A. Whitehead, W. Querbes, J.R. Dorkin, J. Qin, W. Cantley, L.L. Qin, T. Racie, M. Frank-Kamenetsky, K.N. Yip, R. Alvarez, D.W. Sah, A. de Fougerolles, K. Fitzgerald, V. Koteliensky, A. Akinc, R. Langer, D.G. Anderson, Lipid-like materials for low-dose, in vivo gene silencing, *Proc. Natl. Acad. Sci. U. S. A.* 107 (2010) 1864–1869.
- [10] S.C. Semple, A. Akinc, J. Chen, A.P. Sandhu, B.L. Mui, C.K. Cho, D.W. Sah, D. Stebbing, E.J. Crosley, E. Yaworski, I.M. Hafez, J.R. Dorkin, J. Qin, K. Lam, K.G. Rajeev, K.F. Wong, L.B. Jeffs, L. Nechev, M.L. Eisenhardt, M. Jayaraman, M. Kazem, M.A. Maier, M. Srinivasulu, M.J. Weinstein, Q. Chen, R. Alvarez, S.A. Barros, S. De, S.K. Klimuk, T. Borland, V. Kosovrasti, W.L. Cantley, Y.K. Tam, M. Manoharan, M.A. Ciufolini, M.A. Tracy, A. de Fougerolles, I. MacLachlan, P.R. Cullis, T.D. Madden, M.J. Hope, Rational design of cationic lipids for siRNA delivery, *Nat. Biotechnol.* 28 (2010) 172–176.
- [11] S. Chono, S.D. Li, C.C. Conwell, L. Huang, An efficient and low immunostimulatory nanoparticle formulation for systemic siRNA delivery to the tumor, *J. Control. Release* 131 (2008) 64–69.
- [12] A. Akinc, A. Zumbuehl, M. Goldberg, E.S. Leshchiner, V. Busini, N. Hossain, S.A. Bacallado, D.N. Nguyen, J. Fuller, R. Alvarez, A. Borodovsky, T. Borland, R. Constien, A. de Fougerolles, J.R. Dorkin, K. Narayanannair Jayaprakash, M. Jayaraman, M. John, V. Koteliensky, M. Manoharan, L. Nechev, J. Qin, T. Racie, D. Raitcheva, K.G. Rajeev, D.W. Sah, J. Soutschek, I. Toudjarska, H.P. Vornlocher, T.S. Zimmermann, R. Langer, D.G. Anderson, A combinatorial library of lipid-like materials for delivery of RNAi therapeutics, *Nat. Biotechnol.* 26 (2008) 561–569.
- [13] M. Damen, J. Aarbiou, S.F. van Dongen, R.M. Buijs-Offerman, P.P. Spijkers, M. van den Heuvel, K. Kvashnina, R.J. Nolte, B.J. Scholte, M.C. Feiters, Delivery of DNA and siRNA by novel gemini-like amphiphilic peptides, *J. Control. Release* 145 (2010) 33–39.
- [14] M. Mevel, N. Kamaly, S. Carmona, M.H. Oliver, M.R. Jorgensen, C. Crowther, F.H. Salazar, P.L. Marion, M. Fujino, Y. Natori, M. Thanou, P. Arbuthnot, J.J. Youanc, P.A. Jaffres, A.D. Miller, DODAG: a versatile new cationic lipid that mediates efficient delivery of pDNA and siRNA, *J. Control. Release* 143 (2010) 222–232.
- [15] Y. Nakamura, K. Kogure, S. Futaki, H. Harashima, Octaarginine-modified multifunctional envelope-type nano device for siRNA, *J. Control. Release* 119 (2007) 360–367.
- [16] M.S. Suh, G. Shim, H.Y. Lee, S.E. Han, Y.H. Yu, Y. Choi, K. Kim, I.C. Kwon, K.Y. Weon, Y.B. Kim, Y.K. Oh, Anionic amino acid-derived cationic lipid for siRNA delivery, *J. Control. Release* 140 (2009) 268–276.
- [17] U.K. Laemmli, Characterization of DNA condensates induced by poly(ethylene oxide) and polylysine, *Proc. Natl. Acad. Sci. U. S. A.* 72 (1975) 4288–4292.
- [18] F.C. MacLaughlin, R.J. Mumper, J. Wang, J.M. Tagliaferri, I. Gill, M. Hinchcliffe, A.P. Rolland, Chitosan and depolymerized chitosan oligomers as condensing carriers for in vivo plasmid delivery, *J. Control. Release* 56 (1998) 259–272.
- [19] O. Boussif, F. Lezoualch, M.A. Zanta, M.D. Mergny, D. Scherman, B. Demeneix, J.P. Behr, A versatile vector for gene and oligonucleotide transfer into cells in culture and in vivo: polyethylenimine, *Proc. Natl. Acad. Sci. U. S. A.* 92 (1995) 7297–7301.
- [20] H.-j.P. Junghun Suh, Hwang Byung Keun, Ionization of Poly(ethyleneimine) and Poly(allylamine) at Various pH's, *Bioorg. Chem.* 22 (1994) 318–327.
- [21] J.P. Behr, B. Demeneix, J.P. Loeffler, J. Perez-Mutul, Efficient gene transfer into mammalian primary endocrine cells with lipopolyamine-coated DNA, *Proc. Natl. Acad. Sci. U. S. A.* 86 (1989) 6982–6986.
- [22] M.A. Dobrovolskaia, P. Aggarwal, J.B. Hall, S.E. McNeil, Preclinical studies to understand nanoparticle interaction with the immune system and its potential effects on nanoparticle biodistribution, *Mol. Pharm.* 5 (2008) 487–495.
- [23] J. Heyes, L. Palmer, K. Bremner, I. MacLachlan, Cationic lipid saturation influences intracellular delivery of encapsulated nucleic acids, *J. Control. Release* 107 (2005) 276–287.
- [24] A. Santel, M. Aleku, O. Keil, J. Endruschat, V. Esche, G. Fisch, S. Dames, K. Loffler, M. Fechtner, W. Arnold, K. Giese, A. Klippel, J. Kaufmann, A novel siRNA-lipoplex technology for RNA interference in the mouse vascular endothelium, *Gene Ther.* 13 (2006) 1222–1234.
- [25] S.-D.L. Sumio Chono, Christine C. Conwell, Huang Leaf, An efficient and low immunostimulatory nanoparticle formulation for systemic siRNA delivery to the tumor, *J. Control. Release* 131 (2008) 64–69.
- [26] R.E. Vandenbroucke, I. Lentacker, J. Demeester, S.C. De Smedt, N.N. Sanders, Ultrasound assisted siRNA delivery using PEG-siPlex loaded microbubbles, *J. Control. Release* 126 (2008) 265–273.

- [27] B.M. Kinsey, C.L. Densmore, F.M. Orson, Non-viral gene delivery to the lungs, *Curr. Gene Ther.* 5 (2005) 181–194.
- [28] C. Marchini, M. Montani, A. Amici, H. Amenitsch, C. Marianecci, D. Pozzi, G. Caracciolo, Structural stability and increase in size rationalize the efficiency of lipoplexes in serum, *Langmuir* 25 (2009) 3013–3021.
- [29] T. Gjetting, N.S. Arildsen, C.L. Christensen, T.T. Poulsen, J.A. Roth, V.N. Handlos, H.S. Poulsen, In vitro and in vivo effects of polyethylene glycol (PEG)-modified lipid in DOTAP/cholesterol-mediated gene transfection, *Int J Nanomedicine* 5 (2010) 371–383.
- [30] J.K. Kim, S.H. Choi, C.O. Kim, J.S. Park, W.S. Ahn, C.K. Kim, Enhancement of polyethylene glycol (PEG)-modified cationic liposome-mediated gene deliveries: effects on serum stability and transfection efficiency, *J. Pharm. Pharmacol.* 55 (2003) 453–460.
- [31] J. Heyes, K. Hall, V. Taylor, R. Lenz, I. MacLachlan, Synthesis and characterization of novel poly(ethylene glycol)-lipid conjugates suitable for use in drug delivery, *J. Control. Release* 112 (2006) 280–290.
- [32] K.J. Polach, M. Matar, J. Rice, G. Slobodkin, J. Sparks, R. Congo, A. Rea-Ramsey, D. McClure, E. Brunhoeber, M. Krampert, A. Schuster, K. Jahn-Hofmann, M. John, H.P. Vornlocher, J.G. Fewell, K. Anwer, A. Geick, Delivery of siRNA to the mouse lung via a functionalized lipopolyamine, *Mol. Ther.* (2011). doi:10.1038/mt.2011.210.